NANO LETTERS

Letter

pubs.acs.org/NanoLett

Wafer-Scale Fabrication of Plasmonic Crystals from Patterned Silicon Templates Prepared by Nanosphere Lithography

Anthony Shoji Hall, Stuart A. Friesen, and Thomas E. Mallouk*

Department of Chemistry, The Pennsylvania State University, 104 Chemistry Building, University Park, Pennsylvania 16802, United States

Supporting Information

ABSTRACT: By combining nanosphere lithography with template stripping, silicon wafers were patterned with hexagonal arrays of nanowells or pillars. These silicon masters were then replicated in gold by metal evaporation, resulting in wafer-scale hexagonal gratings for plasmonic applications. In the nanosphere lithography step, two-dimensional colloidal crystals of 510 nm diameter polystyrene spheres were assembled at the air−water interface and transferred to silicon wafers. The spheres were etched in oxygen plasma in order to define their size for masking of the silicon wafer. For fabrication of metallic nanopillar arrays, an alumina film was grown over the nanosphere layer and the spheres were then removed by bath sonication. The well pattern was defined in the silicon wafer by reactive ion etching in a chlorine plasma. For fabrication of metal nanowell arrays, the nanosphere monolayer was used directly as a mask and exposed areas of the silicon wafer were plasma-etched anisotropically in SF_6/Ar. Both techniques could be used to produce subwavelength metal replica structures with controlled pillar or well diameter, depth, and profile, on the wafer scale, without the use of direct writing techniques to fabricate masks or masters.

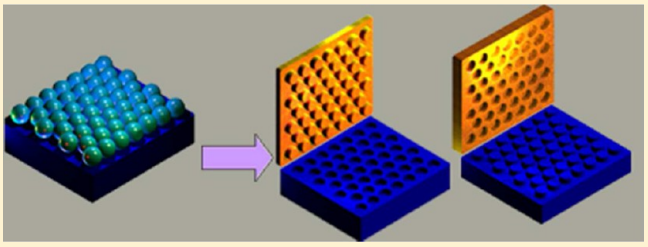

KEYWORDS: *Self-assembly, nanosphere lithography, plasmonics, surface plasmon polariton, light trapping, nanophotonics, plasmonic crystals, gratings, diffraction gratings*

The fabrication of plasmonic nanostructures such as metallic gratings has recently garnered much attention due the ability of such structures to concentrate and guide light.[1] Subwavelength confinement of light leads to enhanced absorption by semiconductors or by light-absorbing molecules that are positioned near the metal surface; this resonant phenomenon has motivated the exploration of metallic nanostructures for applications in thin film photovoltaics,[2] photoelectrochemical cells,[3] and biosensors.[4]

The excitation of surface plasmon-polariton (SPP) waves at a flat metal/dielectric interface is forbidden due to the momentum mismatch between the incoming light and the SPP wave.[1] Prism or grating coupling is typically used to provide the momentum balance needed to launch an SPP wave.[2] Subwavelength scale grating couplers are traditionally made by direct-writing methods such as electron beam lithography or focused ion beam milling. The drawback of these techniques is that sample sizes typically range from hundreds of micrometers to a few square millimeters, and much larger structures are too costly or time-consuming to fabricate. Techniques such as nanoimprint,[5] nanostencil lithography,[6] Moiré nanolithography,[7] and soft lithography[8] are useful alternatives for generating larger pattern sizes, but they require direct-writing techniques for fabrication of the master with which the pattern is produced. Nanosphere lithography has also been used to create plasmonic nanostructures through direct assembly of metal nanoparticles,[9−11] or through lift off or direct etching of metals with polymer nanosphere masks. However, for these techniques the templates cannot be reused because the spheres that are deposited serve as a sacrificial mask.[12−20] Template stripping, a technique that uses a single patterned silicon template to prepare hundreds of metallic replicas, has recently emerged as a high throughput method for preparing ultrasmooth plasmonic nanostructures.[19,20] This technique has mainly been used for fabricating grating couplers from silicon masters patterned by electron beam lithography, focused ion beam milling, and optical lithography. Plasmonic nanostructures fabricated by such techniques require a large initial investment for the tools and masks with which to generate wafer-scale patterns. There have been several reports of combining nanosphere lithography and template stripping for fabricating periodic triangle nanoparticle arrays,[21−26] nanodome arrays,[27] and nanopyramid arrays.[28] However these papers have not demonstrated the ability to control depth, filling fraction and profile in metallic gratings fabricated from a polystrene mask of a fixed periodicity. Our recent work on the optimization of metallic gratings for thin film solar cells has shown that the depth (usually 50 nm or deeper) and profile of the metallic gratings are important in enhancing the absorption of light.[29] The preparation of periodic and ultrasmooth grating couplers on a large scale at low cost with precise control over periodicity, profile, filling fraction, and depth is quite challenging by using existing techniques. In this Letter, we demonstrate a simple technique that allows one to fabricate hexagonal

Received: February 28, 2013
Revised: April 14, 2013
Published: April 24, 2013

   dx.doi.org/10.1021/nl400755a | *Nano Lett.* 2013, 13, 2623−2627

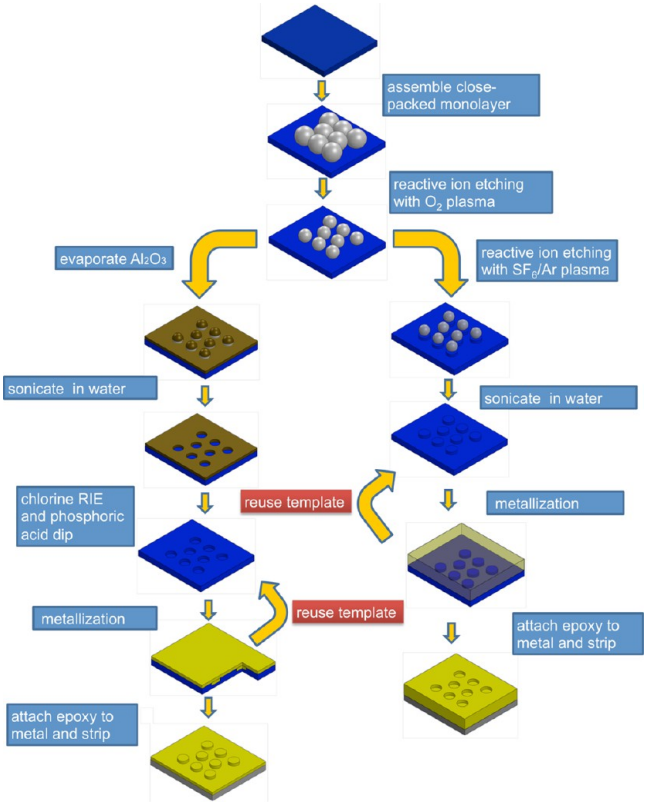

Figure 1. Schematic of the process flow for fabricating metallic nanopillar and nanowell gratings by assembly of a polystyrene sphere monolayer and template stripping.

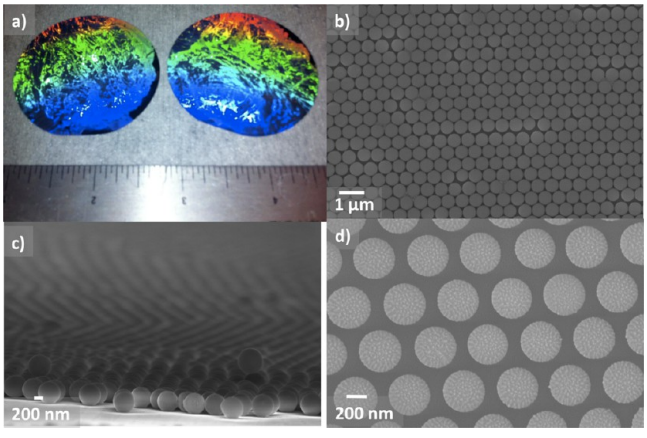

Figure 2. Ordered PS monolayers on 2 in. silicon substrates. (a) Photograph of PS films on a silicon wafer. (b) SEM image of a PS film. (c) Cross sectional SEM image of PS film. (d) SEM image of oxygen-etched PS.

plasmonic gratings at low cost, and without the use of direct writing methods, on the wafer scale with precise control over grating periodicity, profile, filling fraction, and depth.

To create plasmonic nanostructures over large areas, we have combined template stripping with colloidal lithography to fabricate metallic nanopillar and nanowell arrays. A schematic of this process is shown in Figure 1. Close-packed monolayers of 510 nm diameter carboxylate-modified polystyrene spheres (Thermoscientific, W050CA) were deposited on two-inch silicon wafers by shadow nanosphere lithography as described elsewhere.[30,31] The silicon substrate with the polystyrene sphere monolayer was annealed on a hot plate for 30 s at 105 °C to promote the adhesion of the spheres to the substrate. The diameter of the polystyrene spheres was reduced by reactive ion etching (Plasmatherm Versalock ICP-RIE 700) in an oxygen plasma (45 sccm, 90W) as shown in Figure 2. The diameter of the polystyrene beads can be controlled by adjusting the oxygen plasma etching time. It is important to note that if the polystyrene (PS) beads are etched to smaller than 50% of their original size they become porous and noncircular. For fabrication of metallic nanopillar arrays, a 30 nm thick alumina film was then grown by electron beam evaporation (Semicore Evaporator) over the oxygen plasma-etched polystyrene films at 1 Å/s. The polystyrene was removed by bath sonication in water for 15 min. The pattern was defined into the silicon wafer by reactive ion etching in a chlorine plasma (45 sccm) at a power of 100W. Aluminum oxide was chosen as the mask material for this step because it does not etch in pure chlorine plasmas, and this allows one to etch deeply into the silicon wafer if desired.[32] The alumina was then removed by placing the substrate in a bath of concentrated phosphoric acid at 50 °C for 1 h.

For the fabrication of metal nanowell arrays, the oxygen plasma-etched polystyrene nanosphere monolayer was used directly as a mask to define the pattern in the silicon wafer. SF_6/Ar (10 sccm/40 sccm) was chosen to etch the silicon wafer anisotropically because this gas mixture provides good selectivity between silicon and the polystyrene mask. The depth of the silicon master template can be controlled in this step by controlling the SF_6/Ar etch time. In this step is it important not to use chlorine gas for etching due to low selectivity between silicon and polystyrene; the use of chlorine leads to structures with roughened circular edges as shown in Supporting Information Figure SI-2. The polystyrene spheres were removed from the substrate by bath sonication in water for 15 min.

Periodically patterned metallic structures were fabricated by electron beam evaporation of gold over the patterned silicon templates. Degassed Norland Optical Epoxy #71 was drop cast over the metal film and a clean glass slide was placed on top. The epoxy resin was cured by UV irradiation for 30 min and peeled off the silicon template by sliding a razor blade between the slide and silicon wafer. In order to shift the surface plasmon polariton resonance wavelength of the patterned structures into visible range, 100 nm of silica was electron beam evaporated over the templates at 1 Å/s. In numerical simulations of the optical properties of these structures (see below), the silica was assumed to be conformal to the gold nanowells. The patterned silicon templates can be cleaned and reused many times without pattern degradation.[19] Supporting Information Figure SI-1 shows the silicon master template and a wafer-size replica prepared by this technique.

The profile of the features can be controlled by adjusting the etching parameters during sample preparation. As shown in Figure 3a,b, the filling fraction can be controlled by adjusting the diameter of the polystyrene nanospheres during the oxygen reactive ion etching step. Longer etching times yielded wells with smaller diameters, while shorter etching times yielded larger well diameters. In addition, the depth of the gratings can be adjusted by increasing the silicon etching time with SF_6/Ar or Cl_2 to achieve the desired depth. Figure 3a,b shows electron micrographs of gold nanowell gratings with different filling fractions, and Figure 3c,d shows electron micrographs of gold nanopillar gratings. Figure 4 shows AFM height scans and line scans. The data indicate that the patterned gold surface is ultrasmooth. The RMS roughness varied between 0.2−0.8 nm for both samples when measured at various points along the bottom or top of the

dx.doi.org/10.1021/nl400755a | *Nano Lett.* 2013, 13, 2623−2627

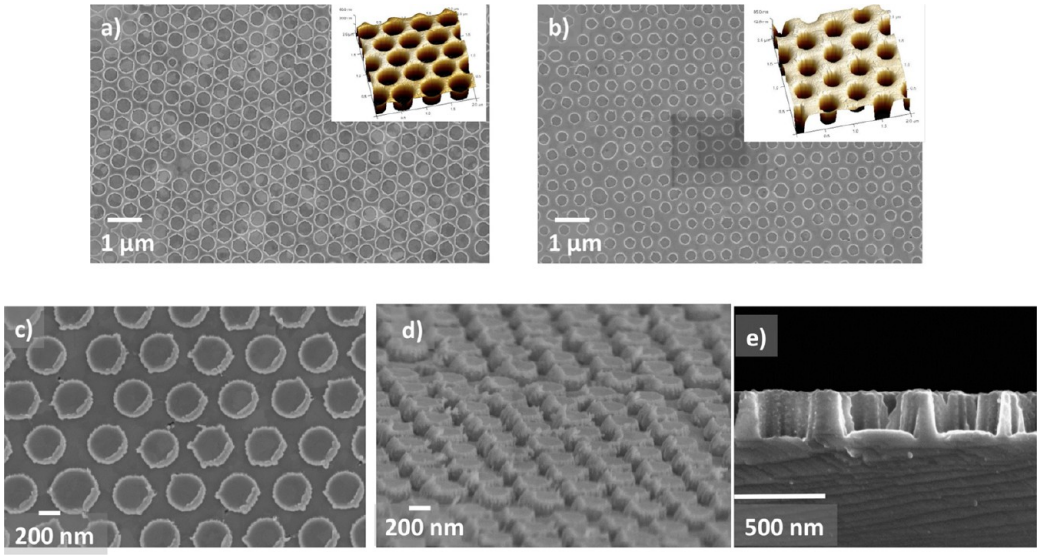

Figure 3. Periodically patterned nanostructures: Gold nanowell grating with (a) large filling fraction and 50 nm depth; (b) small filling fraction and 70 nm depth. (a,b) Insets show 3D AFM images. SEM (c) top-down image of gold nanopillar grating and (d) cross sectional image of the gold nanopillar array shown in (c). (e) A 200 nm deep patterned silicon nanowell master template used to fabricate the gold nanopillar gratings shown in (c,d).

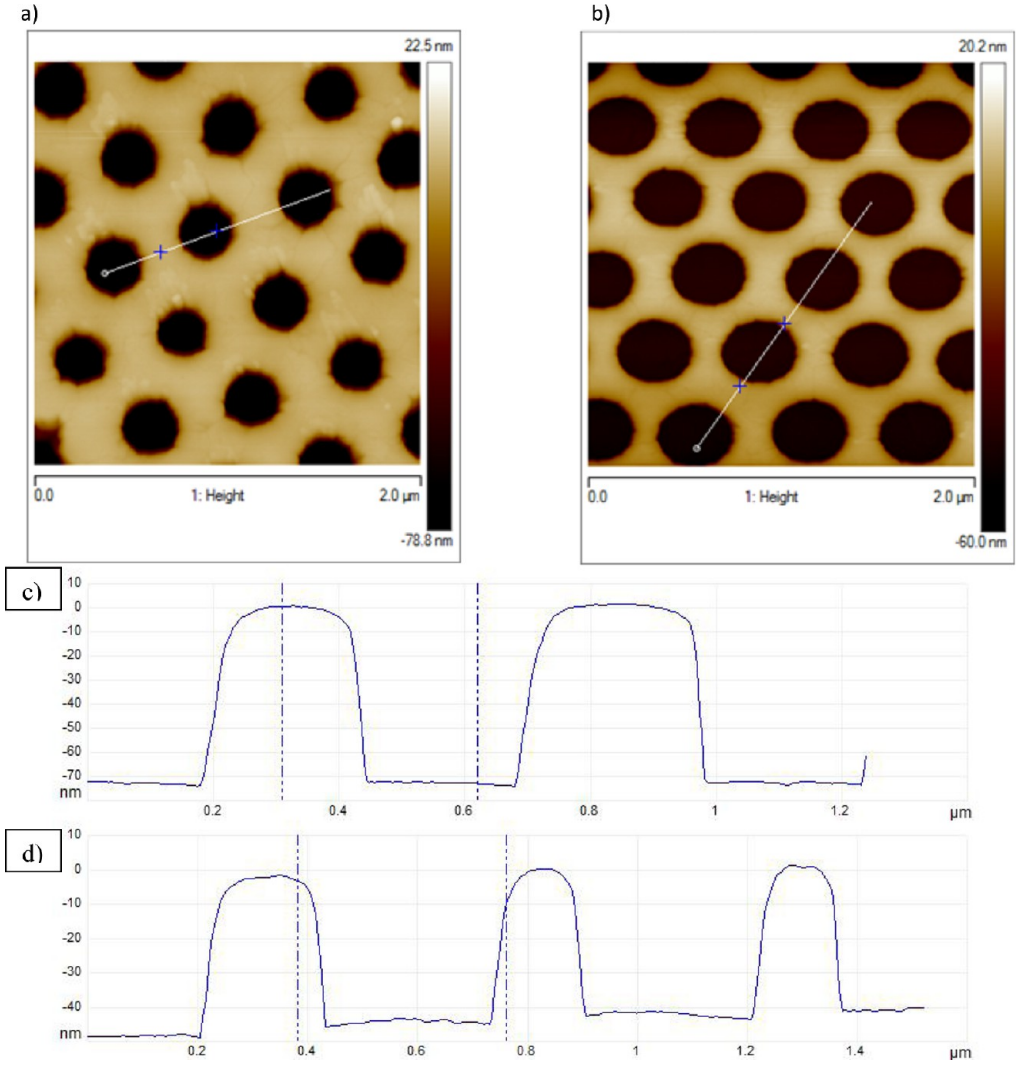

Figure 4. AFM height scans of (a) gold nanowell with small filling fraction. (b) Gold nanowell with large filling fraction. AFM line scans of (c) gold nanowell with small filling fraction. (d) Gold nanowell with large filling fraction. The AFM line scans clearly indicate that the patterned gold possesses ultrasmooth surfaces.

dx.doi.org/10.1021/nl400755a | *Nano Lett.* 2013, 13, 2623−2627

gold nanowell arrays. The patterned metal films made by this technique are derived from polycrystalline 2D colloidal crystals with grain sizes up to a few millimeters, and the metal replicas retain the degree of crystalline order of the template. To test the quality of these metallic films, we measured their specular reflectance with a Perkin-Elmer UV−vis spectrophotometer. Finite difference time domain (FDTD) electromagnetic simulations were performed with Lumerical Solutions FDTD software (Vancouver, Canada) to compare to the reflectance data. In the numerical simulations, Bloch boundary conditions were used in the *x* direction, periodic boundary conditions in the *y* direction, and perfectly matched layers in the *z* direction. The optical constants of silica were taken from the literature.[33] The optical constants of gold was measured by spectroscopic ellipsometry (Woollam RC2 Spectroscopic Ellipsometer) on a planar film and fitted with the appropriate models. A plane-wave source with 45° polarization angle (unpolarized light) and 8° angle of incidence were used. Reflection and transmission were calculated by placing (in the simulation) power monitors 500 nm above and below the structure. Transmission in this structure was found to be negligible, consistent with the optically thick (>100 nm) gold layers. Field distributions were calculated by placing field-profile monitors along specific planes within the unit cell.

The simulated and experimental reflectance of the silica-coated nanowell array imaged in Figure 3b is shown in Figure 5.

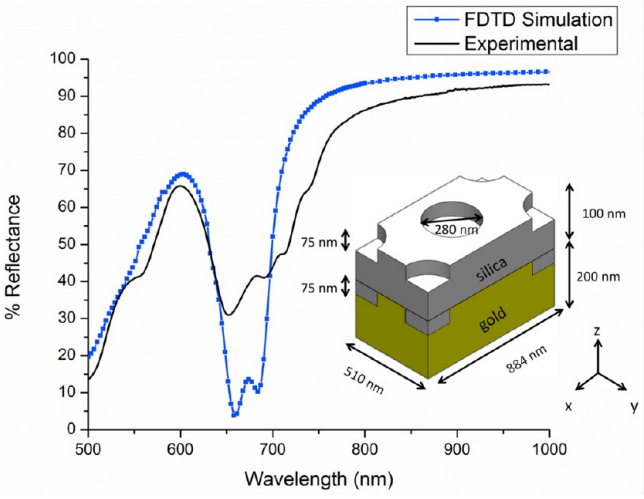

Figure 5. Experimental and simulated reflectivity of a gold nanowell grating with a 100 nm silica overlayer. The inset shows a schematic of the unit cell used in the FDTD simulation.

The resonant wavelengths in the simulated and experimental spectra match well. The sample exhibits multiple resonance peaks. The two most efficiently coupled resonances at 658 nm and 683 nm have coupling efficiencies of ca. 70 and 60%, respectively. The multiple peaks observed in this structure are caused by Fabry−Perot interference effects between reflected SPP waves within the nanowell.[34] The peaks in the experimental data are less intense and broader due to some randomization induced by the defects and grain boundaries of the polycrystalline colloidal template and resulting replica pattern.[35] Figure 6b,c shows the calculated electric field profile of a cross section that passes through the center of the middle of the *ZY* plane of the unit cell, at λ_o = 658 nm and λ_o = 683 nm. The sharp points of the nanowell display the largest field enhancements in the structure. An interference pattern caused by a partially reflected SPP wave

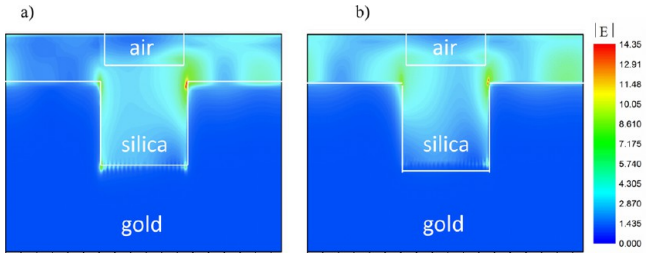

Figure 6. Calculated electric field intensity in the middle of the unit cell through the *ZY* plane nanowell array at (a) λ_o = 658 nm and (b) λ_o = 683 nm. These diagrams are not plotted to scale.

is observed at the bottom of the well. The evanescent decay of the field intensity away from the metal surface provides further evidence that the reflectance dips are caused by the excitation of SPP waves.[1]

In summary, we have demonstrated a scalable, high throughput method for preparing two-dimensional metallic grating couplers for plasmonic applications. The technique combines elements of both nanosphere lithography and template stripping, which together provide a means of producing masters and replica plasmonic nanostructures inexpensively and on the wafer scale. It should be possible to trap light in different wavelength ranges by changing the size of the PS beads that define the period of the grating. Nagpal et al. have shown that such silicon templates can be used many times without noticeable degradation in the metal replicas.[19] We investigated the plasmonic properties of a test structure and successfully demonstrated that metallic gratings fabricated by this technique exhibit interesting plasmonic reflectance properties that are consistent with FDTD simulations. Gratings fabricated by this method may be useful for enhancing the efficiency of photovoltaics and in other applications where large-area, inexpensive light-trapping structures are needed.

■ ASSOCIATED CONTENT

Supporting Information

Additional information and figures. This material is available free of charge via the Internet at http://pubs.acs.org.

■ AUTHOR INFORMATION

Corresponding Author

*E-mail: tem5@psu.edu.

Notes

The authors declare no competing financial interest.

■ ACKNOWLEDGMENTS

We thank Julie Anderson and Melisa Yashinski for assistance with electron microscopy. This work was supported by the National Science Foundation under Grant DMR-1125591. Support for the Penn State Nanofabrication Laboratory is provided in part by the National Science Foundation under Cooperative Agreement ECS-0335765.

■ REFERENCES

(1) Maier, S. A. Plasmonics—Fundamentals and Applications; Springer: New York, 2007.

(2) Atwater, H. A.; Polman, A. A. Plasmonics for improved photovoltaic devices. *Nat. Mater.* **2010**, *9*, 205−213.

(3) Nishijima, Y.; et al. Near-infrared plasmon-assisted water oxidation. *J. Phys. Chem. Lett.* **2012**, 3, 1248−1252.

(4) Homola, J.; Yee, S. S.; Gauglitz, G. Surface plasmon resonance sensors: review. *Sens. Actuators, B* **1999**, *54*, 3−15.

(5) Boltasseva, B. Plasmonic components fabrication via nanoimprint. *J. Opt. A: Pure Appl. Opt.* **2009**, *11*, 114001.
(6) Malyarchuk, V.; Hua, F.; Mack, N. H.; Velasquez, V. T.; White, J. O.; Nuzzo, R. G.; Rogers, J. A. High performance plasmonic crystal sensor formed by soft nanoimprint lithography. *Opt. Exp.* **2005**, *13*, 5669−5675.
(7) Lee, M.; Lin, J. Y.; Odom, T. W. Large-area nanocontact printing using metallic nanostencil masks. *Angew. Chem., Int. Ed.* **2010**, *49*, 3057−3060.
(8) Lubin, S. M.; Zhou, W.; Hryn, A. J.; Huntington, M. D.; Odom, T. W. High rotational symmetry lattices fabricated by Moiré nanolithography. *Nano Lett.* **2012**, *12*, 4948−4952.
(9) Eguchi, M.; Mitsui, D.; Wu, H.-L.; Sato, R.; Teranishi, T. Simple reductant concentration-dependent shape control of polyhedral gold nanoparticles and their plasmonic properties. *Langmuir* **2012**, *28*, 9021.
(10) Swanglap, P.; Slaughter, L. S.; Chang, W.-S.; Willingham, B.; Khanal, B. P.; Zubarev, E. R.; Link, S. Seeing double:coupling between substrate image charges and collective plasmon modes in self-assembled nanoparticle superstructures. *ACS Nano* **2011**, *5*, 4892−4901.
(11) Desireddy, A.; Joshi, C. P.; Sestak, M.; Little, S.; Kumar, S.; Podraza, N. J.; Marsillac, S.; Collins, R. W.; Bigioni, T. P. Wafer-scale self-assembled plasmonic thin films. *Thin Solid Films* **2011**, *519*, 6077−6084.
(12) Haynes, C. L.; Van Duyne, R. P. Nanosphere Lithography: A versatile nanofabrication tool for studies of size-dependent nanoparticle optics. *J. Phys. Chem. B* **2001**, *105*, 5599−5611.
(13) Zheng, Y. B.; Juluri, B. K.; Mao, X.; Walker, T. R.; Huang, T. J. Systematic investigation of localized surface plasmon resonance of long-range ordered au nanodisk arrays. *J. Appl. Phys.* **2008**, *103*, 014308.
(14) Zheng, Y. B.; Juluri, B. K.; Kiraly, B.; Huang, T. J. Ordered Au Nanodisk and Nanohole Arrays: Fabrication and Applications. *J. Nanotechnol. Eng. Med.* **2010**, *1*, 31011.
(15) Fredriksson, H.; Alaverdyan, Y.; Dmitriev, A.; Langhammer, C.; Sutherland, D. S.; Zäch, M.; Kasemo, B. Hole−mask colloidal lithography. *Adv. Mater.* **2007**, *19*, 4297−4302.
(16) Tsuboi, Y.; Shoji, T.; Kitamura, N.; Takase, M.; Murakoshi, K.; Mizumoto, Y. Optical trapping of quantum dots based on gap-mode-excitation of localized surface plasmon, Ishihara, H. *J. Phys. Chem. Lett.* **2010**, *1*, 2327−2333.
(17) Lin, M.-H.; Chen, H.-Y.; Gwo, S. Layer-by-layer assembly of three-dimensional colloidal supercrystals with tunable plasmonic properties. *J. Am. Chem. Soc.* **2010**, *132*, 11259−11263.
(18) Saracut, V.; Giloan, M.; Gabor, M.; Astilean, S.; Farcau, C. Polarization-Sensitive Linear Plasmonic Nanostructures via Colloidal Lithography with Uniaxial Colloidal Arrays. *ACS Appl. Mater. Interfaces* **2013**, *5*, 1362−9.
(19) Nagpal, P.; Lindquist, N. C.; Oh, S. H.; Norris, D. J. Ultrasmooth patterned materials for plasmonics and metamaterials. *Science* **2009**, *325*, 594−597.
(20) Wang, K.; Schonbrun, E.; Steinvurzel, P.; Crozier, K. B. Trapping and rotating nanoparticles using a plasmonic nano-tweezer with an integrated heat sink. *Nat. Commun.* **2011**, *2*, 1480/1−6.
(21) Yu, J.; Geng, C.; Zheng, L.; Ma, Z.; Tan, T.; Wang, T.; Yan, Q.; Shen, D. Preparation of High-Quality Colloidal Mask for Nanosphere Lithography by a Combination of Air/Water Interface Self-Assembly and Solvent Vapor Annealing. *Langmuir* **2012**, *28*, 12681−12689.
(22) Retsch, M.; Tamm, M.; Bocchio, N.; Horn, N.; Forch, R.; Jonas, U.; Kreiter, M. Fabrication of Nanoscale Rings, Dots, and Rods by Combining Shadow Nanosphere Lithography and Annealed Polystyrene Nanosphere Masks. *Small* **2009**, *5*, 2105−2110.
(23) Wright, J. P.; Worsfold, O.; Whitehouse, C.; Himmelhaus, M. Ultraflat Ternary Nanopatterns Fabricated using Colloidal Lithography. *Adv. Mater.* **2006**, *18*, 421−426.
(24) Jung, B.; Frey, W. Large-scale ultraflat nanopatterned surfaces without template residues. *Nanotechnology* **2008**, *19*, 145303.
(25) Vogel, N.; Jung, M.; Retsch, M.; Knoll, W.; Jonas, U.; Koper, I. Laterally Patterned Ultraflat Surfaces. *Small* **2009**, *5*, 821−825.
(26) Vogel, N.; Jung, M.; Bocchio, N. L.; Retsch, M.; Kreiter, M.; Koper, I. Reusable Localized Surface Plasmon Sensors Based on Ultrastable Nanostructures. *Small* **2010**, *6*, 104−109.
(27) Frey, W.; Woods, C. K.; Chilkoti, A. Ultraflat nanosphere lithography: A new method to fabricate flat nanostructures. *Adv. Mater.* **2000**, *12*, 1515.
(28) Sun, C. H.; Linn, N. C.; Jiang, P. Templated Fabrication of Periodic Metallic Nanopyramid Arrays. *Chem. Mater.* **2007**, *19*, 4551−4556.
(29) Solano, M.; Faryad, M.; Hall, A. S.; Mallouk, T. E.; Monk, P. B.; Lakhtakia, A. Optimization of the absorption efficiency of a thin-film tandem solar cell backed by a metallic surface relief grating. *Appl. Opt.* **2013**, *52*, 966−979.
(30) Kandulski, W. *Shadow Nanosphere Lithography*. Ph.D. Dissertation, Bonn University, Bonn, Germany, 2007.
(31) Kosiorek, A.; Kandulski, W.; Chudzinski, P.; Kempa, K.; Giersig, M. Shadow nanosphere lithography: simulation and experiment. *Nano Lett.* **2004**, *4*, 1359−1363.
(32) Oh, J. R.; Moon, J. H.; Park, H. K.; Park, J. H.; Chung, H.; Jeong, J.; Kim, W.; Do, Y. R. Wafer-scale colloidal lithography based on self-assembly of polystyrene nanospheres and atomic layer deposition. *J. Mater. Chem.* **2010**, *20*, 5025−5029.
(33) Lynch, D. W.; Hunter, W. R. In *Handbook of Optical Constants of Solids*; Palik, E. D., Ed.; Academic Press: New York, 1985; pp 350−356.
(34) Artar, A.; Yanik, A. A.; Altug, H. Fabry−Pérot nanocavities in multilayered plasmonic crystals for enhanced biosensing. *Appl. Phys. Lett.* **2009**, *95*, 051105.
(35) Yoshiaki, N.; Rosa, L.; Juodkazis, S. Surface plasmon resonances in periodic and random patterns of gold nano-disks for broadband light harvesting. *Opt. Exp.* **2012**, *20*, 11466−11477.